START 0000058

DECEMBER 1973 HY12

JOURNAL OF THE
HYDRAULICS DIVISION

Saturated-Unsaturated Seepage by Finite Elements

By Shlomo P. Neuman[1]

Introduction

Traditionally, civil engineers have tended to focus their attention on the saturated zone in analyzing seepage through earth structures and the subsurface. However, unsaturated flow plays an important role in a large number of engineering problems, e.g., the movement of toxic leachates beneath sanitary landfills takes place largely under unsaturated conditions. Similar conditions often prevail during the percolation of clear or polluted water from surface bodies such as rivers, ditches, and canals toward the ground-water table. Freeze (4) showed that seepage through earth dams under variable reservoir heads cannot be validly investigated without taking into account the unsaturated zone. An understanding of flow in this zone is also important for stability analyses because negative pore-water pressures cannot be calculated by using the classical free-surface approach. Unsaturated flow conditions are also encountered in dealing with unconfined aquifers, watershed hydrology, irrigation, and the drainage of agricultural lands.

The problems of fluid flow in unsaturated porous media lead to quasilinear partial differential equations that are very difficult to solve by analytical methods. With the advent of high-speed digital computers during the last two decades, approximate numerical techniques have been applied to an increasing degree in solving such problems. Most of these methods were developed by soil scientists who favored the conventional finite difference approach. A comprehensive review

Note.—Discussion open until May 1, 1974. To extend the closing date one month, a written request must be filed with the Editor of Technical Publications, ASCE. This paper is part of the copyrighted Journal of the Hydraulics Division, Proceedings of the American Society of Civil Engineers, Vol. 99, No. HY12, December, 1973. Manuscript was submitted for review for possible publication on June 8, 1973.

[1]Sr. Sci., Inst. of Soils and Water, Agr. Research Organization, The Volcani Center, Bet Dagan, Israel.

NOTICE: This material may be protected by copyright law (Title 17 U.S. Code)

of this approach as well as a complete survey of all pertinent literature were given by the writer in a previous report (1).

Due to the limitations of the usual finite difference approach, there has been in recent years a shift of emphasis, especially in civil engineering, toward the development of more powerful numerical techniques based on the concepts of variational calculus. These new techniques, commonly known as the finite element method, have already been successfully applied to many fluid flow problems (2,5,6,7,10,11,12,14,15,16,17,18,19).

In the present work an iterative Galerkin-type finite element method is used to solve the equations of transient seepage in saturated-unsaturated porous media. The resulting computer program is capable of handling nonuniform flow regions having complex boundaries and arbitrary degrees of local anisotropy. Flow can take place in a vertical plane, in a horizontal plane, or in a three-dimensional system with radial symmetry. Boundary conditions that vary with time in a prescribed stepwise fashion are conveniently treated with this program. When one or more seepage faces are present, their locations are automatically adjusted at each time step. The soil is allowed to be slightly compressible and this is taken into account indirectly through the concept of effective formation compressibility. Experience with the finite element algorithm indicates that convergence of the iterative scheme is near quadratic in many cases. A listing of the computer program is available elsewhere (9). Two examples, one of infiltration into an earth dam with a sloping core, and the other of flow through a layered medium cut by a complex topography, are also included in the text.

Governing Partial Differential Equations

The following analysis is written in an indicial notation whereby quantities with a single subscript (or index) represent components of vectors, and quantities with two subscripts are components of second rank matrices or tensors. When an index appears twice in any given term of an algebraic expression, this term must be summed over all admissible values of that particular index.

The equation of continuity for an infinitesimal element of the porous medium can be written in terms of macroscopic quantities as

$$-\frac{\partial}{\partial x_i}(\rho v_i) = \frac{\partial}{\partial t}(\rho \phi S_w) \quad \text{(1)}$$

in which ρ = the density of water; v_i = the Darcy velocity or specific flux; ϕ = the porosity; and S_w = the degree of volumetric water saturation ($0 \leq S_w \leq 1$). From Darcy's law one has

$$v_i = -K^s_{ij} K_r \frac{\partial h}{\partial x_j} \quad \text{(2)}$$

in which K_r = the relative hydraulic conductivity ($0 \leq K_r \leq 1$); and h = the hydraulic head. Eq. 2 assumes that the hydraulic conductivity can be expressed as the multiple of a symmetric positive-definite tensor, K^s_{ij}, representing the conductivity at saturation, and a scalar function of the degree of saturation, $K_r(S_w)$. This representation need not be strictly correct but it may be presently justified in view of our limited knowledge about the functional relationship

between K_{ij} and S_w. Substituting Eq. 2 into Eq. 1 leads to

$$\frac{\partial}{\partial x_i}\left(\rho K_{ij}^s K_r \frac{\partial h}{\partial x_j}\right) = \frac{\partial}{\partial t}(\rho \phi S_w) \quad (3)$$

The term on the right-hand side of Eq. 3 can be expanded by adopting an argument similar to that of Cooley (3). Let c_f be the formation compressibility defined as

$$c_f \doteq \frac{1}{\phi}\frac{\partial \phi}{\partial p} = \frac{1}{\rho g \phi}\frac{\partial \phi}{\partial h} \quad (4)$$

in which p = the pore-water pressure; and ϕ = the volume of voids per unit volume of porous material. The idea of expressing the compressibility in terms of fluid pressure instead of effective stress is derived from ground-water hydrology and petroleum engineering practice. This can be justified provided that the total stress is fixed at each point and the deformation is elastic and vertical. In shallow soils where the total stress is strongly affected by surface loads and by overlying changes in the state of saturation, c_f must be viewed merely as an effective formation compressibility and its application is limited to a narrow range of variations in the state of stress. Under unsaturated conditions where the relationship between total stress, effective stress, and fluid pressure is a function of S_w, c_f may change considerably from its saturated value. However, the effect of soil compressibility on the storage of water under unsaturated conditions is usually quite small relative to the effect of changes in S_w, and therefore c_f can be safely neglected.

By expanding the right-hand side in Eq. 3 and assuming that spatial variations in ρ are negligibly small owing to the slight compressibility of water, the flow equation becomes

$$\frac{\partial}{\partial x_i}\left(K_{ij}^s K_r \frac{\partial h}{\partial x_j}\right) = \phi \frac{\partial S_w}{\partial t} + S_w S_s \frac{\partial h}{\partial t} \quad (5)$$

in which the specific storage, S_s, is defined as

$$S_s = \rho g \phi (c_w + c_f) \quad (6)$$

and c_w = the compressibility of water.

For practical purposes, it is often convenient to express Eq. 6 in terms of the pressure head, ψ, and the volumetric moisture content, θ, rather than in terms of h and S_w. If one defines the specific moisture capacity, C, as

$$C = \frac{\partial \theta}{\partial \psi} \quad (7)$$

then Eq. 5 can be rewritten in the form

$$\frac{\partial}{\partial x_i}\left(K_r K_{ij}^s \frac{\partial \psi}{\partial x_j} + K_r K_{i3}^s\right) = \left(C + \frac{\theta}{\phi} S_s\right)\frac{\partial \psi}{\partial t} \quad (8)$$

Since hysteresis is not considered in the present analysis, ψ is a single-valued function of θ and therefore, the initial conditions that are required for any

given problem are simply

$$\psi(x_i, 0) = \psi_0(x_i) \quad (9)$$

In addition to this, one will usually encounter two types of boundary conditions, prescribed pressure head and prescribed flux normal to the boundary. Let the boundary of the flow region, Γ, consist of two types of segments, Γ_1 and Γ_2, such that $\Gamma = \Gamma_1 \cup \Gamma_2$. Then the prescribed pressure head boundary condition can be written as

$$\psi(x_i, t) = \Psi(x_i, t) \quad \text{on} \quad \Gamma_1 \quad (10)$$

and the prescribed flux boundary condition becomes

$$K_r\left(K^s_{ij}\frac{\partial\psi}{\partial x_j} + K^s_{i3}\right)n_i = -V(x_i, t) \quad \text{on} \quad \Gamma_2 \quad (11)$$

in which Ψ and V are prescribed functions of x_i and t; and n_i are the components of the unit outer normal on Γ.

Application of Galerkin Method

Eqs. 8, 9, 10, and 11 are solved by the Galerkin method in conjunction with a finite element discretization scheme. According to the Galerkin method, an approximate solution to this problem at any given instant of time, t, is obtained in the form of a finite sequence:

$$\psi^N(x_i, t) = \psi_n(t)\,\xi_n(x_i); \quad n = 1, 2, \ldots, N \quad (12)$$

in which $\{\xi_n(x_i)\}_{n=1}^N$ is a set of N linearly independent coordinate functions; and $\psi_n(t)$ are time-dependent coefficients yet to be determined. In choosing the coordinate functions, $\psi(x_i, t)$ is assumed to be a square-integrable function (in the Lebesque sense) belonging to a Hilbert space, H. The approximate solution, $\psi^N(x_i, t)$, must belong to an N-dimensional subspace of H, H^N, whose elements satisfy all continuity criteria as well as boundary conditions of the problem. Eq. 12 implies that each element of H^N can be expressed uniquely as a linear combination of all the $\xi_n - s$. Thus, the functions, $\{\xi_n\}_{n=1}^N$, must be chosen so as to constitute a complete set spanning the subspace, H^N, thereby forming a basis for H^N (see Ref. 13).

If R denotes the interior of the flow region over which $\psi(x_i, t)$ is defined, then the norm of ψ, $\|\psi\|$, is obtained from

$$\|\psi\|^2 = \int_R \psi^2\, dR \quad (13)$$

It is said that ψ^N converges in the norm to ψ whenever

$$\lim_{N\to\infty} \|\psi - \psi^N\| = 0 \quad (14)$$

The aim of the variational approach is to determine the coefficients, ψ_n, of ψ^N in such a manner as to ensure convergence in the norm to the true solution. In the finite difference approach one usually requires that his solution converge uniformly over the closure of the entire flow region, $\bar{R}$, where $\bar{R} = R \cup \Gamma$.

Although uniform convergence always implies convergence in the norm while the converse is not necessarily true, convergence in the norm is often faster (8) and this is a distinct advantage of the variational method.

Eq. 8 can be rewritten in the form

$$L(\psi) = \frac{\partial}{\partial x_i}\left(K_r K_{ij}^s \frac{\partial \psi}{\partial x_j} + K_r K_{i3}^s\right) - \left(C + \frac{\theta}{\phi} S_s\right)\frac{\partial \psi}{\partial t} = 0 \quad \ldots\ldots\ldots (15)$$

in which L is a quasilinear differential operator defined on R. The Galerkin method stipulates that in order to determine the coefficients of ψ^N so as to minimize $\| \psi - \psi^N \|$, $L(\psi^N)$ must be orthogonal to each of the N coordinate functions, ξ_n:

$$\Omega_n(\psi^N) = \int_R L(\psi^N)\, \xi_n \, dR = 0; \quad n = 1, 2, \ldots, N \quad \ldots\ldots\ldots\ldots\ldots (16)$$

In other words, the functional, $\Omega_n(\psi^N)$, must vanish for each value of n.

Finite Element Discretization

In using the finite element discretization scheme, the flow region, $\bar{R}$, is subdivided into a network of elements. It is convenient to adopt a network composed of triangular elements for plane flow and a network composed of concentric rings of constant triangular cross section for axisymmetric problems. Let the corners of these elements be designated as nodal points and let x_i^n be the space coordinates of the nth node. Each node, n, is associated with a unique subregion of $\bar{R}$, $\bar{R}^n$, containing all elements in the immediate vicinity of n (see shaded area in Fig. 1). In addition, each node is associated with a global coordinate function, $\xi_n(x_i)$, which is linear in x_i inside each element and piecewise linear over $\bar{R}$, such that

$$\xi_n(x_i^m) = \delta_{nm}, \quad \text{for all} \quad x_i^m \quad \text{in} \quad \bar{R} \quad \ldots\ldots\ldots\ldots\ldots\ldots\ldots (17a)$$

$$\xi_n(x_i) = 0, \quad \text{for all} \quad x_i \quad \text{not in} \quad R^n \quad \ldots\ldots\ldots\ldots\ldots\ldots\ldots (17b)$$

in which δ_{nm} = Kronecker delta (i.e., $\delta_{nm} = 1$ if $n = m$ and $\delta_{nm} = 0$ if $n \neq m$) and R^n = the interior of $\bar{R}^n$.

Owing to their unique shape, ξ_n are sometimes referred to as pyramidal, roof, or chapeau functions. By introducing them into Eq. 12, the latter equation becomes a piecewise linear two-dimensional Lagrange interpolation formula for ψ^N in $\bar{R}$. In other words, the value of ψ^N at any node in $\bar{R}$ is equal to the coefficient, ψ_n, corresponding to that node.

In order to express ξ_n explicitly in terms of the space variables, x_i, it is convenient to consider a single element, $\bar{R}^e$, as shown in Fig. 2. Let $\{\xi_n^e(x_i)\}$ be a set of local coordinate functions that are linear in x_i and satisfy the requirements

$$\xi_n^e(x_i^m) = \delta_{nm}, \quad \text{for all} \quad x_i^m \quad \text{in} \quad \bar{R}^e \quad \ldots\ldots\ldots\ldots\ldots\ldots\ldots (18a)$$

$$\xi_n^e(x_i) = 0, \quad \text{for all} \quad x_i \quad \text{not in} \quad \bar{R}^e \quad \ldots\ldots\ldots\ldots\ldots\ldots\ldots (18b)$$

This together with Eq. 17 implies that the global coordinate functions, ξ_n, are the union of the local coordinate functions, ξ_n^e

$$\xi_n(x_i) = \bigcup_e \xi_n^e(x_i) \quad \ldots \quad (19)$$

in which the union sign is taken over all elements, e. The relationship between ξ_n^e and x_i is given in Appendix I.

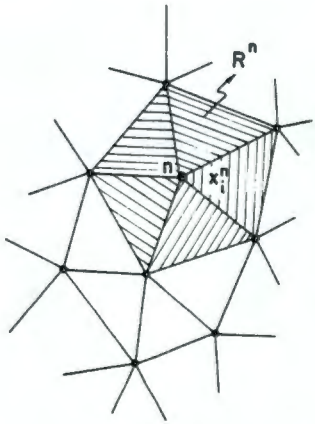

FIG. 1.—Network of Triangular Elements

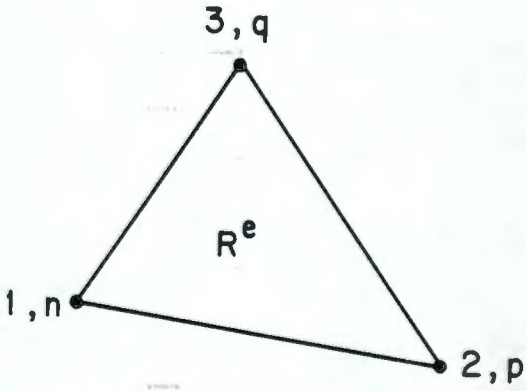

FIG. 2.—Single Triangular Element

By virtue of Eq. 19 it is now possible to rewrite the global functional from Eq. 16, $\Omega_n(\psi^N)$, in terms of equivalent local functionals over individual triangles, $\Omega_n^e(\psi^N)$, so that

$$\Omega_n(\psi^N) = \Omega_n(\psi_m \xi_m) = \Omega_n\left[\psi_m\left(\bigcup_e \xi_m^e\right)\right] = \sum_e \Omega^e{}_n(\psi_m \xi_m^e) = 0 \quad \ldots \quad (20)$$

in which the summation is taken over all elements and

$$\Omega_n^e(\psi_m \xi_m^e) = \int_{R^e} L(\psi_m \xi_m^e)\, \xi_n^e \, dR \quad \ldots \quad (21)$$

Since the Galerkin method applies only at a given instant of time, the time derivative, $\partial\psi/\partial t$, appearing in $L(\psi)$ must be determined independently of the orthogonalization process. Experience indicates that for the numerical method to converge in the case of unsaturated flow, $\partial\psi/\partial t$ must not be replaced by $\partial\psi^N/\partial t$. A much more stable solution is obtained by defining the nodal values of the time derivatives, $\partial\psi_n/\partial t$, as weighted averages of $\partial\psi/\partial t$ over the entire flow region, R:

$$\frac{\partial\psi_n}{\partial t} \equiv \frac{\int_R \left(C + \frac{\theta}{\phi} S_s\right) \frac{\partial\psi}{\partial t} \xi_n \, dR}{\int_R \left(C + \frac{\theta}{\phi} S_s\right) \xi_n \, dR} \quad \text{(22)}$$

The physical meaning of this definition will be explained later. In addition to this, it is assumed that K^s_{ij}, ϕ, and S_s are constant in each element, while K_r, C, and θ vary linearly according to

$$K_r = K_{rl}\,\xi^e_l \quad \text{(23 a)}$$

$$C = C_l\,\xi^e_l \quad \text{(23 b)}$$

$$\theta = \theta_l\,\xi^e_l \quad \text{(23 c)}$$

in which l stands for the corners of the triangle.

By combining Eqs. 20, 21, 22, and 23, and using Green's first identity, one obtains a set of quasilinear first-order differential equations

$$\mathbf{A}_{nm}\psi_m + \mathbf{F}_{nm}\frac{\partial\psi_m}{\partial t} = Q_n - B_n; \quad n, m = 1, 2, \ldots, N \quad \text{(24)}$$

in which, for a vertical cross section

$$\left.\begin{aligned} \mathbf{A}_{nm} &= \sum_e K_{rl} K^s_{ij} \int_{R^e} \xi^e_l \frac{\partial\xi^e_n}{\partial x_i}\frac{\partial\xi^e_m}{\partial x_j} dR \\ \mathbf{A}_{nm} &= \sum_e \frac{\alpha}{4\Delta} \bar{K}_r [K^s_{11} b_n b_m + K^s_{13}(b_n c_m + b_m c_n) + K^s_{33} c_n c_m] \end{aligned}\right\} \quad \text{(25 a)}$$

$$\left.\begin{aligned} \mathbf{F}_{nn} &= \sum_e \int_{R^e} \left(C_l \xi^e_l + \frac{S_s}{\phi}\theta_l \xi^e_l\right) \xi^e_n \, dR \\ \mathbf{F}_{nn} &= \sum_e \frac{\alpha\Delta}{12}\left[(2C_n + C_p + C_q) + \frac{S_s}{\phi}(2\theta_n + \theta_p + \theta_q)\right] \end{aligned}\right\} \quad \text{(25 b)}$$

$$\mathbf{F}_{nm} = 0, \quad \text{if} \quad n \neq m \quad \text{(25 c)}$$

$$Q_n = -\sum_e \int_{\Gamma^e} V \xi^e_n \, d\Gamma = -\sum_e \alpha \frac{(LV)_n}{2} \quad \text{(25 d)}$$

$$B_n = \sum_e K_{rl} K^s_{i3} \int_{R^e} \xi^e_l \frac{\partial\xi^e_n}{\partial x_i} dR = \sum_e \frac{\alpha}{2} \bar{K}_r (K^s_{i3} b_n + K_{33} c_n) \quad \text{(25 e)}$$

The subscripts, n, p, and q, refer to the three corners of each triangle as shown in Fig. 2; Δ = the area of the triangle; $\alpha = 1$ for plane flow and $\alpha = 2\pi\bar{x}_1$ for axisymmetric flow; $\bar{x}_1$ is the average horizontal (or radial) coordinate given by $\bar{x}_1 = [(x_1)_n + (x_1)_p + (x_1)_q]/3$; $\bar{K}_r$ = the average relative conductivity given by $\bar{K}_r = (K_{rn} + K_{rp} + K_{rq})/3$; and b and c are geometric coefficients defined in Appendix I. The term, $(LV)_n$, represents the flow rate across any side of the triangle, of length L, which includes nodal point n. The V value is assumed to be uniform along L.

In the case of horizontal plane flow, $\mathbf{B}_n$ must be set equal to zero for all values of n. Note that the matrix, $\mathbf{A}_{nm}$, is sparse and symmetric while $\mathbf{Q}_n$ is zero at all internal nodal points that do not act as sinks or sources.

Also note that $\mathbf{F}_{nm}$ is a diagonal matrix and this is a direct consequence of the averaging process implied by Eq. 22. The physical meaning of this averaging process is now evident: $\mathbf{F}_{nn}$ is the amount of water stored in the entire flow system when the value of ψ at node n changes by one unit in unit time. Thus, $\mathbf{F}_{nn}$ is a global coefficient of storage corresponding to nodal point n. According to Eq. 25b, the contribution of each triangle to $\mathbf{F}_{nn}$ is calculated by giving two times more weight to the values of C and θ at node n than to their values at all other nodes. In the particular case in which C and θ are uniform inside an element, the storage capability of the element is equally divided between its three corner nodes so that $\mathbf{F}_{nn}$ represents one third the storage capability of this element.

Extension to Quadrilateral Elements

The diagonal shape of $\mathbf{F}_{nm}$ enables one to employ quadrilateral elements in addition to triangular elements. Consider a typical quadrilateral element as shown in Fig. 3 and let its corner nodes be numbered locally from 1 to 4. By designating a fifth nodal point at the center of the quadrilateral, the latter can be subdivided into four triangles. Obviously, each of the five nodes is associated with one equation of the type given in Eq. 24. However, the equation corresponding to the center can be eliminated as will be shown.

If one wants to treat the quadrilateral as a single element with four nodes, its contribution to $\mathbf{F}_{nn}$ can be derived by analogy to the triangle. This contribution must be such that the weight given to C and θ at node n is twice as large as that given to them at the remaining three nodes. In addition, when C and θ are uniform over the entire quadrilateral, the storage capability of the element must be divided equally between the four corner nodes, so that each node is associated with one fourth of the total value. Thus, the contribution of a quadrilateral to $\mathbf{F}_{nn}$ is

$$\frac{\alpha\nabla}{20}\left[(2C_n + C_p + C_q + C_r) + \frac{S_s}{\phi}(2\theta_n + \theta_p + \theta_q + \theta_r)\right] \quad \ldots\ldots\ldots (26)$$

in which n, p, q, and r represent the corner nodes; ∇ = the area of the quadrilateral; and α is the same as before except that now $\bar{x}_1 = [(x_1)_n + (x_1)_p + (x_1)_q + (x_1)_r]/4$. Consequently, $\mathbf{F}_{nn}$ for the center point becomes zero.

If the center point is neither a source nor a sink, $Q_5 = 0$; otherwise, it

is possible to divide the value of Q_5 equally between the four corner nodes and then set $Q_5 = 0$. The net result is that Eq. 24 for the center node becomes (since $F_{55} = 0$)

$$A_{51}\psi_1 + A_{52}\psi_2 + A_{53}\psi_3 + A_{54}\psi_4 + A_{55}\psi_5 = -B_5 \quad \text{(27)}$$

This can be solved explicitly for ψ_5 and the result inserted into the equations corresponding to the four corner nodes. In this manner, the size of the matrix, A_{nm}, is greatly reduced without impairing its symmetric nature.

Obviously, each triangle can also be divided into three smaller elements and the equation for the midpoint can be eliminated in a similar fashion. While

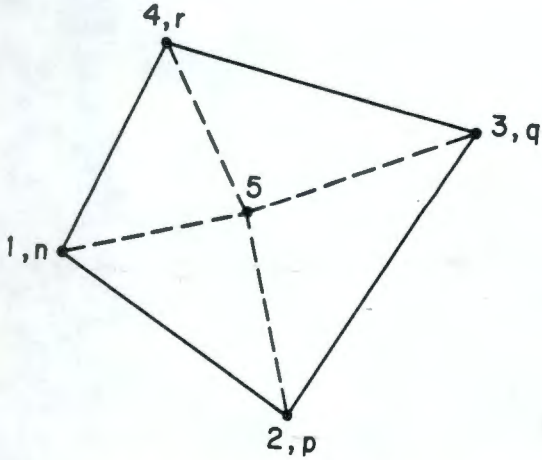

FIG. 3.—Single Quadrilateral Element

the size of the matrix, A_{nm}, remains unchanged, the accuracy of the results improves significantly.

Integration Over Time

To integrate Eq. 24, the time domain is discretized into a sequence of finite intervals, Δt, and the time derivatives of ψ_n are replaced by finite differences. If the entire flow system remains unsaturated at all times, good results can be obtained by employing the time-centered scheme

$$\left[A_{nm}^{k+(1/2)} + \frac{2}{\Delta t_k} F_{nm}^{k+(1/2)}\right]\psi_m^{k+1} = 2Q_n^{k+(1/2)} - 2B_n^{k+(1/2)} - \left[A_{nm}^{k+(1/2)} - \frac{2}{\Delta t_k} F_{nm}^{k+(1/2)}\right]\psi_m^k; \quad n, m = 1, 2, \ldots, N \quad \text{(28)}$$

in which k represents the time; $t = t_k$; and $\Delta t_k = t_{k+1} - t_k$. In order to evaluate the coefficients in Eq. 28, one must know the values of $\psi_n^{k+(1/2)}$ at $t_{k+(1/2)} = t_k + \Delta t_k/2$. At the beginning of each time step, these are predicted by linear extrapolation from previously calculated values according to

$$\psi_n^{k+(1/2)} = \psi_n^k + \frac{\Delta t_k}{2\Delta t_{k-1}}(\psi_n^k - \psi_n^{k-1}) \quad \ldots \quad (29)$$

The resulting set of simultaneous linear algebraic equations is then solved by a highly efficient Gauss elimination algorithm for the values of ψ_n^{k+1} at all nodes.

Due to the nonlinear nature of Eq. 28, these results must be improved by an iterative process. At each iteration, the most recent values of ψ_n^{k+1} are used to obtain an improved estimate of $\psi_n^{k+(1/2)}$ from

$$\psi_n^{k+(1/2)} = \frac{1}{2}(\psi_n^k + \psi_n^{k+1}) \quad \ldots \quad (30)$$

After having reevaluated the coefficients, the equations are again solved by Gaussian elimination for improved values of ψ_n^{k+1}. The iterative procedure continues as long as it is necessary to achieve a satisfactory degree of convergence.

Note that by employing Gaussian elimination simultaneously over the entire finite element network, the iterative process is fully implicit and is therefore very fast. This form of iteration is sometimes referred to as the method of simultaneous displacements. Since experience indicates that near-quadratic convergence can be achieved in many cases, this approach offsets all the well-known deficiencies of the Gaussian elimination scheme. Moreover, this approach appears to be superior to the Newton-Raphson method which relies on a complex nonsymmetric matrix and is highly sensitive to the initial estimate of $\psi_n^{k+(1/2)}$ during each time step.

The time-centered scheme can also be used in systems that do not remain completely unsaturated, provided that S_s in the saturated region is not zero. If S_s is zero and part of the system is saturated, the values of F_{nn} in the saturated zone vanish, and the governing equations there become elliptic. This means that sudden changes in boundary conditions around the saturated zone have an instantaneous effect on the values of ψ everywhere in this zone, so that ψ is no longer a continuous function of time. For example, by imposing a certain boundary condition at time $t = t_k$, all values of ψ in the saturated zone change instantaneously and the values of ψ_n^k at the start of the time step, Δt_k, become unknown. Thus, the right-hand side of Eq. 28 is unknown, and the equations cannot be solved.

To overcome this problem, one must adopt a fully implicit backward difference scheme in terms of ψ:

$$\left[A_{nm}^{k+(1/2)} + \frac{1}{\Delta t_k} F_{nm}^{k+(1/2)}\right]\psi_m^{k+1} = Q_n^{k+(1/2)} - B_n^{k+(1/2)}$$

$$+ \frac{1}{\Delta t_k} F_{nm}^{k+(1/2)} \psi_m^k \quad \ldots \quad (31)$$

Here the coefficients are still evaluated at half the time step, $k + (1/2)$, and this is done in order to dampen the tendency of ψ to oscillate around its limit. Such oscillations are frequently encountered in highly nonlinear systems such as the one dealt with herein and a well-known method of overcoming this problem is to employ under-relaxation techniques. The effect of evaluating the coefficients

at half the time step is to under-relax the system.

When S_s is zero, the global storage coefficient, F_{nn}, vanishes in the saturated zone and one can obtain a solution without knowing the values of ψ_n^k at the start of the time step in this zone. The only exception to this rule occurs at nodes that pass from a state of saturation to a state of incomplete saturation during a time step. The values of $F_{nn}^{k+(1/2)}$ corresponding to such nodes may differ from zero and Eq. 31 can no longer be solved without knowing the values of ψ_n^k. However, since $S_s = 0$, $F_{nn}^{k+(1/2)}$ now represents only storage due to changes in the moisture content, θ. Such changes occur only within the negative range of ψ values but when ψ is positive, $C = \partial\theta/\partial\psi$ is zero. Thus, whenever a value of ψ_n^k in the saturated zone becomes unknown due to a sudden change in the boundary conditions, one is justified in replacing this value by zero in Eq. 31.

Treatment of Seepage Faces

A seepage face is an external boundary of the saturated zone where water leaves the system and ψ is uniformly zero. Under transient conditions, the length of the seepage face varies with time in a manner that cannot be predicted a priori. If one treats the seepage face as a prescribed pressure head boundary with $\psi = 0$, the length of this face remains fixed, and this is contrary to the physics of transient flow. On the other hand, the seepage face cannot be treated as a prescribed flux boundary because the values of Q_n there are generally unknown. How, then, should a seepage face be treated?

To answer this question, reference is made to all nodes which, at any stage of the calculation, can belong to a given seepage face by having zero values of ψ_n and negative values of Q_n (recall that Q_n is negative when the flow at node n is directed out of the system). Suppose that, knowing the position of the seepage face at time t_k, it is desired to predict its position at time t_{k+1}. During the first iteration, ψ is set equal to zero along the initial length of the seepage face and the latter is treated as a prescribed ψ boundary. At the same time, Q is set equal to zero at all nodes with $\psi < 0$ and this segment is treated as a prescribed flux boundary. The solution is expected to yield negative values of Q at nodes where ψ is prescribed to be zero, and negative values of ψ at nodes where Q is prescribed to be zero. If, instead, a positive value of Q is encountered at a node where $\psi = 0$, the value of Q there is set equal to zero and, in the next iteration, this node is treated as a prescribed flux boundary. On the other hand, if a positive value of ψ is encountered at a node where $Q = 0$, the value of ψ there is set equal to zero and, in the next iteration, this node is treated as a prescribed pressure head boundary. Experience has shown that in order for the solution to converge, this modification of the boundary conditions should always procede sequentially from node to node, starting at the saturated end of the seepage face. In addition, after having set Q equal to zero at any node during a given iteration, Q at all the subsequent nodes must also be set equal to zero. The iterative process continues in the manner described earlier until a sufficient degree of convergence is achieved at each node in the network.

Note that due to the ease with which prescribed flux boundary conditions are treated in the finite element method, the handling of seepage faces is

considerably simpler than with the finite difference approach.

Examples and Conclusions

All the features described in the foregoing have been incorporated into a computer program that is able to handle both plane and axisymmetric flow. The functional relationships between ψ, θ, and K_r are obtained by linear interpolation between discrete values. Details of the computer program are available elsewhere (9). The following examples have been carefully chosen to illustrate the power of the finite element approach and to demonstrate the

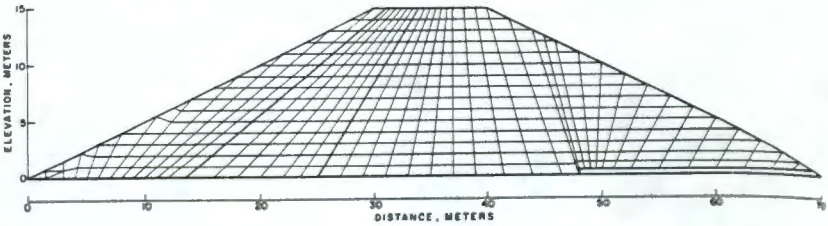

FIG. 4.—Earth Dam with Finite Element Network

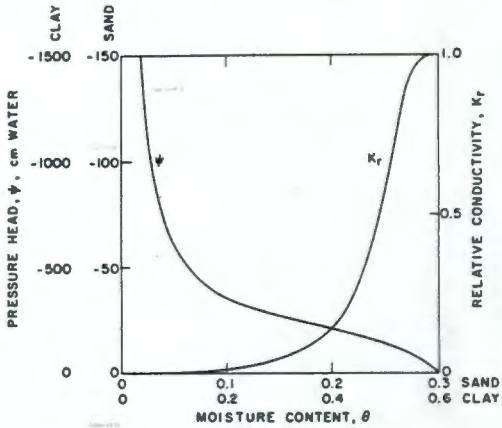

FIG. 5.—Variation of ψ and K_r with Moisture Content for Two Soils

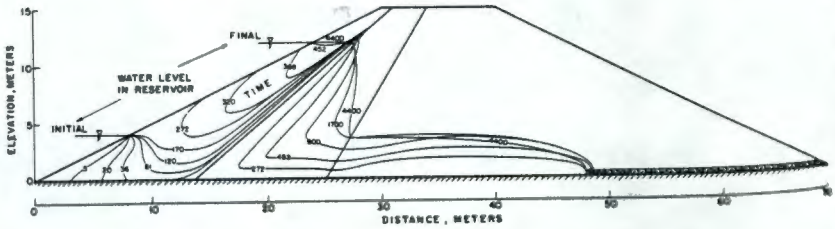

FIG. 6.—Advance of Zero Pressure Surface in Earth Dam

importance of unsaturated flow. The results are expressed in terms of arbitrary time units.

The first example is that of transient seepage through an earth dam with a sloping core and a horizontal drain. A cross section of the dam, together with the superimposed finite element network, are shown in Fig. 4. The saturated hydraulic conductivity of the sandy shell material is 0.5 cm per unit time in the horizontal direction and 0.1 cm per unit time in the vertical direction. The saturated conductivity of the clay core is 0.0001 cm per unit time in the horizontal direction and 0.001 cm per unit time in the vertical direction. Fig. 5 shows the variation of ψ and K_r with moisture content for both materials. The value of S_s is zero and the effect of surface loads on the pore pressure is neglected.

In engineering practice, earth dam fills are usually compacted at near-saturated moisture contents. In the present example, the initial value of θ is 0.255 in

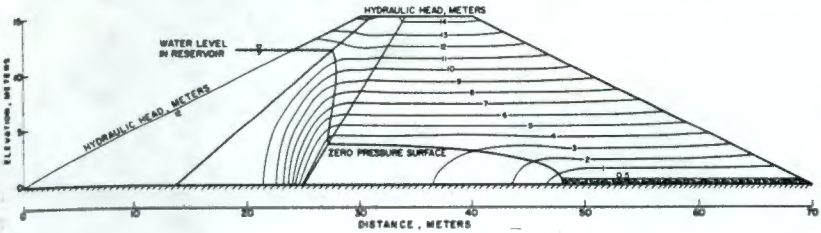

FIG. 7.—Contours of Equal Hydraulic Head in Earth Dam at t = 4,400

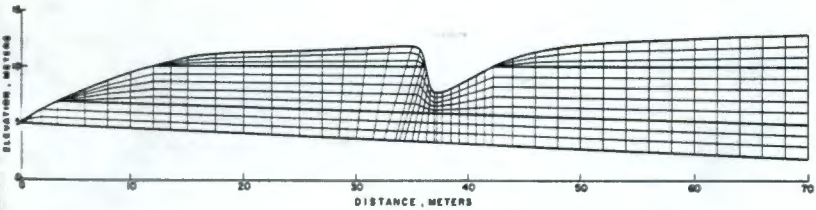

FIG. 8.—Hill-Slope with Finite Element Network

the shell and 0.598 in the core. The boundary of the porous material along the drain is treated as a potential seepage face. At time t = 0, the water level in the reservoir is suddenly raised to an elevation of 4 m and this situation is maintained for a period of 182 time units. This is followed by a gradual rise in the water level at a rate of 1 m per 24 time units until the reservoir reaches an elevation of 12 m at t = 374. After this time, the water level in the reservoir remains at a constant elevation of 12 m above the impervious base.

Fig. 6 shows the advance of the zero pressure (i.e., ψ = 0) surface which, in the present case, separates between the saturated and the unsaturated portions of the dam. In the classical approach this is considered to be a moving material boundary and is usually referred to as free surface (12). As one can see in Fig. 6, the zero pressure surface may have an inverted shape and this situation

cannot be handled with the classical approach. In addition, the rate of advance of this surface is strongly affected by antecedent moisture conditions in the unsaturated zone (4) and therefore this rate cannot always be correctly predicted with the free surface approach.

Fig. 6 presents some interesting features of saturated-unsaturated flow regime in an earth dam. Since the initial moisture content is uniform in each segment of the dam, the pressure head is also uniform, indicating that a vertical hydraulic gradient must exist in the unsaturated zone. This gradient results in the accumulation of water on the upstream face of the clay core and in the formation of a saturated mound at the bottom of the downstream shell. As time goes on, the rate of moisture content redistribution in the unsaturated zone diminishes, and the mound as well as all excess water above the clay core slowly dissipate. At time $t = 4{,}400$, the zero pressure surface attains a quasisteady configuration, and flow in the saturated zone reaches a state of near-equilibrium. However, nonequilibrium conditions still prevail in the unsaturated zone, and this is shown in Fig. 7.

Fig. 7 shows contours of equal hydraulic head in the dam at $t = 4{,}400$. These contours demonstrate the existence of a hydraulic gradient causing downward flow in the unsaturated zone. Although the example has not been carried beyond 4,400 time units, there is sufficient evidence to indicate that the contours will continue to recede upward and will rotate in a counterclockwise fashion until the final steady state is reached. At this stage, the upper and downstream boundaries of the dam will become flow lines and some water from the reservoir will continue to flow through the unsaturated zone.

It is interesting to note that the interface between the porous material and the horizontal drainage blanket acts like an impermeable boundary at $t = 0$, but later two seepage faces develop, one along the vertical wall on the left and one near the toe of the dam on the right. At $t = 150$, the two seepage faces become one, and this situation remains permanent. Thus, much of the water that seeps into the drain is derived from the overlying unsaturated zone. This is consistent with the laws of physics because the interface itself is saturated and maintains a pressure of zero, thereby constituting a constant hydraulic head boundary as is indicated in Fig. 7.

Freeze (Ref. 4, p. 937) claims that ". . . classical saturated analyses for full drainage blankets, which treat the horizontal interface between dam and filter as a seepage face, must . . . be in error" and suggests the replacement of the drain by a highly permeable porous material. The present analysis does not support Freeze's viewpoint.

The second example is that of seepage through a layered hill-slope cut by a ditch. A cross section of the slope, together with the superimposed finite element network, are shown in Fig. 8. The principal values of the saturated hydraulic conductivities in each of the three layers, in centimeters per unit time, are given in Fig. 9. The variation of ψ and K_r with moisture content for the bottom clay layer and the two overlying sandy layers are the same as in Fig. 5, S_s is 10^{-4} inverse meters in the bottom layer and zero in the overlying layers.

Prior to the time, $t = 0$, the ditch is empty and the system is under a quasi-steady state. Flow takes place from right to left and water leaves the system through two seepage faces, one along the ditch and the other along the slope. At time

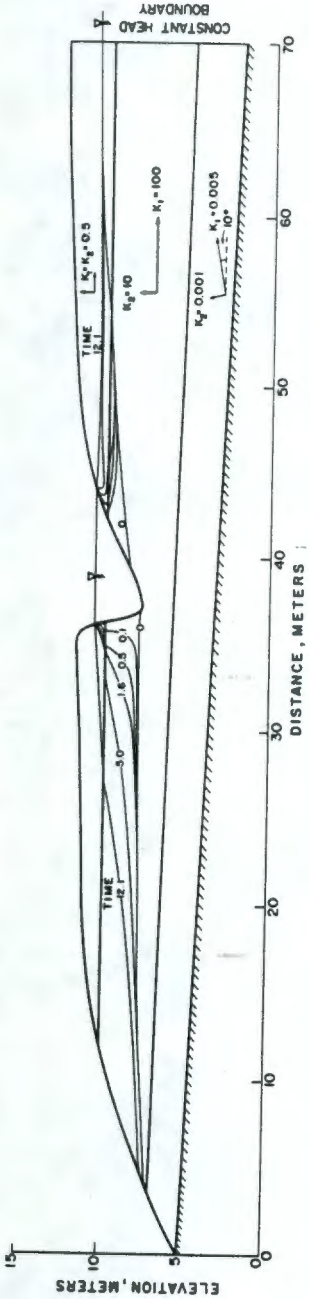

FIG. 9.—Advance of Zero Pressure Surface in Hill-Slope

$t = 0$, the ditch suddenly fills with water to a level of 10.7 and this situation is maintained indefinitely.

Fig. 9 shows the advance of the zero pressure surface up to the time, $t = 12.1$. It is seen that at early time, the $\psi = 0$ surface is again inverted, and therefore the free surface approach is unsuitable for this problem.

From the present study it can be concluded that the finite element method is well suited for the analysis of transient saturated-unsaturated flow through porous media. The classical approach in which the water table is treated as a moving material interface is limited in its application and it may often lead to erroneous results. Additional research is needed to develop field methods for determining the functional relationships between pressure head, relative conductivity, and moisture content under unsaturated conditions.

Acknowledgment

This investigation was supported in part by grant No. FG-Is-287 made by the United States Department of Agriculture under PL 480 to the Technion, Israel Institute of Technology, Haifa, Israel. The paper is a contribution from the Volcani Center, Agricultural Research Organization, Bet Dagan, Israel, 1973 Series number 277-E.

Appendix I.—Local Coordinate Functions

Referring to Fig. 2, the relationship between local coordinate functions and global Cartesian coordinates in a vertical cross section is obtained directly from Eq. 18:

$$\begin{bmatrix} 1 \\ x_1 \\ x_3 \end{bmatrix} = \begin{bmatrix} 1 & 1 & 1 \\ x_1^1 & x_1^2 & x_1^3 \\ x_3^1 & x_3^2 & x_3^3 \end{bmatrix} \begin{bmatrix} \xi_1^e \\ \xi_2^e \\ \xi_3^e \end{bmatrix} \quad \text{(32)}$$

The inverse of Eq. 32 is

$$\begin{bmatrix} \xi_1^e \\ \xi_2^e \\ \xi_3^e \end{bmatrix} = \frac{1}{2\Delta} \begin{bmatrix} a_1 & b_1 & c_1 \\ a_2 & b_2 & c_2 \\ a_3 & b_3 & c_3 \end{bmatrix} \begin{bmatrix} 1 \\ x_1 \\ x_3 \end{bmatrix} \quad \text{(33)}$$

in which the area of the triangle, Δ, is given by

$$\Delta = \begin{vmatrix} 1 & x_1^1 & x_3^1 \\ 1 & x_1^2 & x_3^2 \\ 1 & x_1^3 & x_3^3 \end{vmatrix} = b_1 c_2 - c_1 b_2 \quad \text{(34)}$$

$$\left.\begin{aligned} &\text{and} \quad a_1 = x_1^2 x_3^3 - x_1^3 x_3^2; \quad b_1 = x_3^2 - x_3^3; \quad c_1 = x_1^3 - x_1^2 \\ &a_2 = x_1^3 x_3^1 - x_1^1 x_3^3; \quad b_2 = x_3^3 - x_3^1; \quad c_2 = x_1^1 - x_1^3 \\ &a_3 = x_1^1 x_3^2 - x_1^2 x_3^1; \quad b_3 = x_3^1 - x_3^2; \quad c_3 = x_1^2 - x_1^1 \end{aligned}\right\} \quad \text{(35)}$$

In addition $$\frac{\partial \xi_n^e}{\partial x_1} = \frac{b_n}{2\Delta}; \quad \frac{\partial \xi_n}{\partial x_3} = \frac{c_n}{2\Delta} \qquad (36)$$

Appendix II.—References

1. Braester, C., et al., "A Survey of the Equations and Solutions of Unsaturated Flow in Porous Media," *First Annual Report, Project No. A10-SWC-77*, Hydraulic Engineering Laboratory, Technion, Haifa, Israel, 1971, p. 176.
2. Cavendish, J. C., Price, H. S., and Varga, R. S., "Galerkin Methods for the Numerical Solution of Boundary Value Problems," *Society of Petroleum Engineers Journal*, Vol. 9, No. 2, 1969, pp. 204–220.
3. Cooley, R. L., "A Finite Difference Method for Unsteady Flow in Variably Saturated Porous Media: Application to a Single Pumping Well," *Water Resources Research*, Vol. 7, No. 6, 1971, pp. 1607–1625.
4. Freeze, R. A., "Influence of the Unsaturated Flow Domain on Seepage Through Earth Dams," *Water Resources Research*, Vol. 7, No. 4, 1971, pp. 929–941.
5. Javandel, I., and Witherspoon, P. A., "Application of the Finite Element Method to Transient Flow in Porous Media," *Society of Petroleum Engineers Journal*, Vol. 8, No. 3, 1968, pp. 241–252.
6. Javandel, I., and Witherspoon, P. A., "A Method of Analyzing Transient Fluid Flow in Multilayered Aquifers," *Water Resources Research*, Vol. 5, No. 4, 1969, pp. 856–869.
7. McCorquodale, J. A., "Variational Approach to Non-Darcy Flow," *Journal of the Hydraulics Division*, ASCE, Vol. 96, No. HY11, Proc. Paper 7694, Nov., 1970, pp. 2265–2278.
8. Mikhlin, S. G., *Variational Methods in Mathematical Physics*, Pergamon Press, Oxford, England, 1964, p. 584.
9. Neuman, S. P., "Finite Element Computer Programs for Flow in Saturated-Unsaturated Porous Media," *Second Annual Report, Project No. A10-SWC-77*, Hydraulic Engineering Laboratory, Technion, Haifa, Israel, 1972, p. 87.
10. Neuman, S. P., and Witherspoon, P. A., "Finite Element Method of Analyzing Steady Seepage with a Free Surface," *Water Resources Research*, Vol. 6, No. 3, 1970, pp. 889–897.
11. Neuman, S. P., and Witherspoon, P. A., "Variational Principles for Fluid Flow in Porous Media," *Journal of the Engineering Mechanics Division*, ASCE, Vol. 97, No. EM2, Proc. Paper 8023, Apr., 1971, pp. 359–374.
12. Neuman, S. P., and Witherspoon, P. A., "Analysis of Nonsteady Flow with a Free Surface Using the Finite Element Method," *Water Resources Research*, Vol. 7, No. 3, 1971, pp. 611–623.
13. Oden, J. T., *Finite Elements of Nonlinear Continua*, McGraw-Hill Book Co., Inc., New York, N.Y., 1972, p. 432.
14. Price, H. S., Cavendish, J. C., and Varga, R. S., "Numerical Methods of Higher-Order Accuracy for Diffusion-Convection Equations," *Society of Petroleum Engineers Journal*, Vol. 8, No. 3, 1968, pp. 293–303.
15. Sandhu, R. S., and Wilson, E. L., "Finite Element Analysis of Flow in Saturated Porous Elastic Media," *Journal of the Engineering Mechanics Division*, ASCE, Vol. 95, No. EM3, Proc. Paper 6615, June, 1969, pp. 641–652.
16. Taylor, R. L., and Brown, C. B., "Darcy Flow Solutions with a Free Surface," *Journal of the Hydraulics Division*, ASCE, Vol. 93, No. HY2, Proc. Paper 5126, Mar., 1967, pp. 25–33.
17. Volker, R. E., "Nonlinear Flow in Porous Media by Finite Elements," *Journal of the Hydraulics Division*, ASCE, Vol. 95, No. HY6, Proc. Paper 6927, Nov., 1969, pp. 2093–2114.
18. Witherspoon, P. A., Javandel, I., and Neuman, S. P., "Use of the Finite Element Method in Solving Transient Flow Problems in Aquifer Systems," *The Use of Analog and Digital Computers in Hydrology, Publication No. 81*, International Association of Scientific Hydrology, Vol. 2, 1968, pp. 687–698.
19. Zienkiewicz, P., Mayer, P., and Cheung, Y. K., "Solution of Anisotropic Seepage

by Finite Elements," *Journal of the Engineering Mechanics Division*, ASCE, Vol 92, No. EM1, Proc. Paper 4676, Feb., 1966, pp. 111-120.

Appendix III.—Notation

The following symbols are used in this paper:

$C = \partial\theta/\partial\psi$ = specific moisture capacity L^{-1};
$c_f = (1/\phi)(\partial\phi/\partial p)$ = effective formation compressibility, L^2F^{-1};
$c_w = (1/\rho)(\partial\rho/\partial p)$ = water compressibility, L^2F^{-1};
g = acceleration due to gravity, LT^{-2};
$h = x_3 + \psi$ = hydraulic head, L;
$K^s_{ij} = k_{ij}\gamma/\nu$ = saturated hydraulic conductivity tensor, LT^{-1};
K_r = relative hydraulic conductivity, dimensionless;
k_{ij} = intrinsic permeability, L^2;
N = number of nodes in finite element network;
n_i = unit outer normal on Γ, dimensionless;
p = pore-water pressure, FL^{-2};
R = interior of flow region;
$\bar{R} = R \cup \Gamma$ = closure of flow region;
$S_s = \rho g\phi(c_w + c_f)$ = specific storage, L^{-1};
S_w = relative water saturation, dimensionless;
t = time, T;
V = prescribed flux on Γ_2, LT^{-1};
v_i = specific flux, LT^{-1};
x_i = Cartesian coordinate, L;
x_3 = vertical coordinate, L;
$\Gamma = \Gamma_1 \cup \Gamma_2$ = boundary of flow region;
Γ_1 = prescribed pressure head boundary;
Γ_2 = prescribed flux boundary;
γ = unit weight of water, FL^{-3};
Δ = area of triangle, L^2;
δ_{nm} = Kronecker delta;
$\theta = S_w\phi$ = volumetric moisture content, dimensionless;
ν = viscosity of water, FTL^{-2};
$\xi_n = \cup_e \xi^e_n$ = global coordinate function associated with nth node, dimensionless;
ξ^e_n = local coordinate functions associated with nth node, defined in Appendix I, dimensionless;
ρ = mass density of water, FT^2L^{-1};
ϕ = porosity, dimensionless;
Ψ = prescribed pressure head on Γ_2, L;
$\psi = p/(\rho g)$ or $h - x_3$ = pressure head, L; and
∇ = area of quadrilateral, L^2.